Int. J. Multiphase Flow Vol. 14, No. 4, pp. 473–481, 1988
Printed in Great Britain

0301-9322/88 $3.00 + 0.00
Pergamon Press/Elsevier

SIMULATION OF GRANULAR LAYER INVERSION IN LIQUID FLUIDIZED BEDS

M. SYAMLAL[1] and T. J. O'BRIEN[2]

[1]EG&G Washington Analytical Services Center Inc. and [2]U.S. Department of Energy, Morgantown Energy Technology Center, Morgantown, WV 26507-0880, U.S.A.

(*Received* 11 *May* 1987; *in revised form* 18 *April* 1988)

Abstract—A hydrodynamic computer model for describing multiparticle fluidization has been developed. Each group of particles, identical in density and in diameter, is treated as a particulate phase in this model. The computer code solves the mass and momentum balance equations for the fluidizing fluid and for the required number of particulate phases. The model has been used to simulate granular layer inversion in a liquid fluidized bed. This phenomenon occurs during the fluidization of a binary mixture of particles in which the denser particles are smaller. In such a system at low fluid velocities, the larger particles segregate into a top layer; at higher fluid velocities, they sink to form a bottom layer. At intermediate fluid velocities, the extent to which the particles mix is determined by the fluid velocity. The simulation results using the multiparticle code are in good agreement with experimental data on granular layer inversion. It is also shown that under some conditions, a radial segregation pattern exists in addition to the experimentally observed axial segregation pattern.

Key Words: fluidization, particle segregation, multiparticle code, hydrodynamic model, numerical simulation

INTRODUCTION

Most of the hydrodynamic models for fluidization treat the gas and particulates as two interpenetrating fluids (e.g. Gidaspow & Ettehadieh 1983). In its simplest formulation, all the solid particles are considered to be identical, characterized by a mean diameter and density. This, however, does not permit the simulation of some very important fluidization phenomena such as segregation and elutriation, which are caused by differences in particle sizes or densities. To simulate these phenomena, the hydrodynamic theory must be extended to accommodate at least two types of particles, differing in diameter, density, or both. This led Syamlal (1985) to develop a multiparticle computer code that can be used to describe the fluidization of several different types of particles. Although the development of even a single-particle computer code is far from complete, it is believed that numerical explorations using the multiparticle code will aid further understanding of the hydrodynamics of fluidization.

Here we use the multiparticle numerical model to study the "inversion" phenomenon in liquid fluidized beds. This phenomenon occurs during the fluidization of a mixture of two types of particles, of different densities and diameters, with the denser particles of smaller diameter. In such a system, at low fluid velocities, the larger (and less dense) particles segregate at the top of the bed while, at high fluid velocities, they settle to form a segregated layer at the bottom of the bed. At intermediate fluid velocities the particles mix completely. Of course, the exact conditions of mixing and segregation depends upon the size and density ratios.

In recent years, several theoretical and experimental studies have been conducted to elucidate the inversion phenomenon (Van Duijn & Rietema 1982; Moritomi *et al.* 1982, 1986; Epstein & Le Clair 1985; Gibilaro *et al.* 1986). It has been explained, typically, in terms of the bulk densities of the single-component beds: $\rho_{bk} = \epsilon_l \rho_l + \epsilon_k \rho_k$ where ϵ_l and ρ_l are the volume fraction and density of the fluid and ϵ_k and ρ_k are the volume fraction and density of the kth granular phase. As the fluid velocity is increased, the bed expands and, consequently, the bulk density decreases to an extent determined by the diameter and density of the bed material. If a mixture of two types of particles whose individual bulk density vs fluid velocity curves intersect are fluidized, inversion may occur; the inversion velocity is predicted to be the fluid velocity at which the bulk densities are equal. This simple explanation for inversion phenomenon implies a unique inversion velocity for a given fluid–solids system. Experiments, however, show a more complicated behavior; the inversion velocity is dependent upon the overall bed composition (Moritomi *et al.* 1982). Gibilaro

et al. (1986) offered an explanation for this by noting that the bottom layer is a mixture of both of the particles. They argued that, at a given velocity, the composition of the bottom layer will adjust so as to maximize its bulk density. Thus, they were able to quantitatively relate the inversion velocity to the overall bed composition.

THE GOVERNING EQUATIONS

We consider a fluidized system consisting of a binary mixture of particles. The solid particles are of different densities and diameters. Following a suggestion made by Soo (1967), we will consider that particles of identical densities and diameters form a distinct continuum—a particulate phase. Greenspan & Ungarish (1982) have used a similar approach for modeling the settling of a mixture particles of different sizes. Thus, we treat the mixture of two types of particles that differ in diameter and density as two distinct, yet interpenetrating, particulate phases. These particulate phases are each characterized by a mean diameter (d_k) and density (ρ_k). The particle diameters and the particle and the fluid densities are taken to be constants. Note that in all the equations the subscript "k" (= 1, 2 or 3) is used to discriminate between phases; the subscript "$k = 1$" is reserved for the fluid phase.

Although on a particle-size scale, the particles and the fluid do not coexist at a spatial location, the three phases (two particulate and one liquid) can be considered to be interpenetrating continua. The fractions of the volume occupied by each of the phases are denoted by ϵ_k and are defined over a volume much larger than $\max|d_k^3|$ but much smaller than the volume of a computational region. Since the fluid and the two particulates form a saturated mixture,

$$\sum_{k=1}^{3} \epsilon_k = 1. \qquad [1]$$

Now, the equations of motion can be written for each of the phases with the modified densities $\epsilon_k \rho_k$. Since interphase mass transfer does not occur between the phases, the continuity equations are very similar to the single-phase continuity equation and are written as

$$\frac{\partial}{\partial t}(\epsilon_k \rho_k) + \nabla \cdot (\epsilon_k \rho_k \mathbf{V}_k) = 0, \qquad [2]$$

where $\mathbf{V}_k$ is the velocity of the kth phase. The momentum equations are also similar to the inviscid single-phase momentum equations, except for the added interphase momentum transfer terms. The fluid-phase momentum equation is written as

$$\frac{\partial}{\partial t}(\epsilon_1 \rho_1 \mathbf{V}_1) + \nabla \cdot (\epsilon_1 \rho_1 \mathbf{V}_1 \mathbf{V}_1) = -\epsilon_1 \nabla P + \epsilon_1 \rho_1 \boldsymbol{g} + \sum_{j=2}^{3} F_{1j}(\mathbf{V}_j - \mathbf{V}_1) \qquad [3]$$

and the particulate-phase momentum equations are written as

$$\frac{\partial}{\partial t}(\epsilon_k \rho_k \mathbf{V}_k) + \nabla \cdot (\epsilon_k \rho_k \mathbf{V}_k \mathbf{V}_k) = -\epsilon_k \nabla P + \epsilon_k \rho_k \boldsymbol{g} + \sum_{j=1}^{3} F_{kj}(\mathbf{V}_j - \mathbf{V}_k) - \epsilon_k \nabla P_s; \qquad [4]$$

P is the fluid pressure, P_s is a solids pressure and F_{kj} are the interphase momentum transfer terms.

The fluid–particle momentum transfer (drag) terms, are written as

$$F_{1k} = F_{k1} = \frac{3}{4} C_{Dk} \frac{\epsilon_k \rho_1 \epsilon_1}{d_k} |\mathbf{V}_1 - \mathbf{V}_k|. \qquad [5]$$

Syamlal & O'Brien (1988), have shown that the drag coefficient, C_{Dk}, can be related to C_{DS}, the drag coefficient for an isolated sphere, as

$$C_{Dk}(\mathrm{Re}_k, \epsilon_1) = \frac{C_{Ds}\left(\frac{\mathrm{Re}_k}{V_r}\right)}{V_r^2}, \qquad [6]$$

where the function V_r is the ratio of the terminal velocity of a group of particles to that of an isolated particle. Among the several empirical correlations available for V_r, only the following one,

given by Garside & Al-Dibouni (1977), can be written as an explicit function of Re_k and ϵ_1:

$$V_r = 0.5\{A - 0.06\,\mathrm{Re}_k + \sqrt{[0.0036\,\mathrm{Re}_k^2 + 0.12\,\mathrm{Re}_k(2B - A) + A^2]}\}, \quad [7]$$

where

$$A = \epsilon_1^{4.14} \quad [8]$$

and

$$B = \begin{cases} 0.8\epsilon_1^{1.28}, & \epsilon_1 \leqslant 0.85, \\ \epsilon_1^{2.65}, & \epsilon_1 > 0.85. \end{cases} \quad [9]$$

For C_{Ds}, the drag coefficient of an isolated sphere, we have chosen a simple representation developed by Dalla Valle (1948),

$$C_{\mathrm{Ds}}(\mathrm{Re}_k) = \left(0.63 + \frac{4.8}{\sqrt{\mathrm{Re}_k}}\right)^2. \quad [10]$$

The particle Reynolds number, Re_k, is defined as

$$\mathrm{Re}_k = \frac{d_k|\mathbf{V}_1 - \mathbf{V}_k|\rho_1}{\mu_1}, \quad [11]$$

where $|\mathbf{V}_1 - \mathbf{V}_k|$ is the magnitude of the local relative velocity and μ_1 is the fluid viscosity.

The formulation of the drag term, F_{1k}, is dictated by the following consideration, which we call the additivity condition. Suppose that we have a fluidized bed of identical particles. While using a multiparticle model, we have a choice of describing the particles as a single particulate phase of volume fraction ϵ_2 or as several particulate phases whose volume fractions add up to ϵ_2. In the first case, we get a single-particulate momentum equation and, in the latter case, several momentum equations. Clearly, these particulate momentum equations should correctly add up to the single momentum equation of the former case. To ensure this additivity condition, we have made the multiparticle drag terms linear functions of ϵ_k ($k \neq 1$).

A particle–particle friction term must be included in the equations to account for the momentum exchange between the particulate phases. Arastoopour *et al.* (1980), observed that such a term is necessary to show the correct segregation between particles of different sizes in a pneumatic conveyor. An equation for such an interaction in a dilute mixture has been suggested by Soo (1967). A similar expression was also used by Nakamura & Capes (1976). An approximate extension for the momentum transfer between the kth and jth particulate phases in a dense bed,

$$F_{kj} = \frac{\alpha(1+e)\epsilon_k\rho_k\epsilon_j\rho_j(d_k + d_j)^2\left[1 + 3\left(\frac{\epsilon_{kj}}{\epsilon_k + \epsilon_j}\right)^{1/3}\right]}{2(d_k^3\rho_k + d_j^3\rho_j)^2\left[3\left(\frac{\epsilon_{kj}}{\epsilon_k + \epsilon_j}\right)^{1/3} - 1\right]}|\mathbf{V}_{kj}|, \quad [12]$$

was derived by Syamlal (1985). The maximum solids volume fraction of a random closely packed structure, ϵ_{kj}, may be calculated as a function of the diameters, d_k and d_j, and the composition using the following empirical formula devised by Fedors & Landel (1979):

$$\epsilon_{kj} = \begin{cases} [(\Phi_k - \Phi_j) + (1-a)(1-\Phi_k)\Phi_j]\dfrac{[\Phi_k + (1-\Phi_j)\Phi_k]X_k}{\Phi_k + \Phi_j} & \text{for } X_k \leqslant \dfrac{\Phi_k}{[\Phi_k + (1-\Phi_k)\Phi_j]} \\ (1-a)[\Phi_k + (1-\Phi_k)\Phi_j](1-X_k) + \Phi_k & \text{for } X_k \geqslant \dfrac{\Phi_k}{[\Phi_k + (1-\Phi_k)\Phi_j]}, \end{cases} \quad [13]$$

where

$$a = \sqrt{\frac{d_j}{d_k}} \quad (d_k > d_j), \quad [14]$$

Φ_k is the particulate volume fraction of the kth single-particle system at maximum packing and

$$X_k = \frac{\epsilon_k}{(\epsilon_k + \epsilon_j)}. \quad [15]$$

$|\mathbf{V}_{kj}|$ is the magnitude of the interphase relative velocity. Note that [12] does not strictly satisfy the requirements of the additivity condition. We also note that the particle–particle friction term will have only a small influence on the equilibrium distributions, which we intend to calculate here.

To describe the solids stresses, a solids pressure term, P_s, is included in the momentum equation [4]. Gidaspow & Ettehadieh (1983) have noted that such a solids pressure term is necessary in the equations to make the characteristics real and thereby to get a well posed initial value problem. In the absence of a solids pressure term, they found that unrealistically small void fractions were occasionally computed. Gidaspow & Ettehadieh (1983) assumed that the solids pressure is an exponential function of the void fraction, ϵ_l. This assumption was extended to multiparticle systems by Syamlal (1985) as,

$$\nabla P_s = \epsilon_k G(\epsilon_l) \nabla \epsilon_l, \quad [16]$$

where G is given by

$$G(\epsilon_l) = 1.5 \cdot 10^{-3} \exp[500(0.4 - \epsilon_l)]. \quad [17]$$

This expedient does not always prohibit the calculation of unrealistically low void fractions, especially in the simulations of multiparticle systems. We therefore imposed an incompressibility constraint that $\epsilon_l \geq \epsilon_l^*$, the minimum possible void fraction. When this constraint is about to be violated in the computations, the void fraction is held constant at the value of ϵ_l^* and P_s is computed as an independent variable such that it takes the minimum value required to maintain the constraint. Thus P_s takes the place of ϵ_l as an unknown variable. Physically, P_s, the solids pressure term, represents the reaction forces that maintain the incompressibility constraint and is analogous to the pressure in incompressible fluids.

A multiparticle code based on the above set of equations has been developed to describe the flow of solid particles of different types and of a fluid. A finite difference technique is used to solve the equations for time-dependent flow in axisymmetric cylindrical coordinates. The continuity equations and the momentum equations, with the exception of the momentum convection terms, are differenced fully implicitly. The resulting nonlinear algebraic equations are solved iteratively to obtain the distribution of the velocities, pressure and volume fractions in the fluidized bed. The numerical method is an extension of Harlow & Amsden's (1975) method which was subsequently used in the K-FIX code (Rivard & Torrey 1977). Gidaspow & Ettehadieh (1983) used the K-FIX code to develop a fluidization model and the multiparticle code evolved from that model. The details of the numerical technique may be found in Syamlal (1985) and in the K-FIX documentation (Rivard & Torrey 1977).

SIMULATION RESULTS

The experimental conditions of Moritomi *et al.* (1982), were chosen for the computer simulations. These are summarized in table 1. The bed geometry was represented in two dimensions by axisymmetric cylindrical coordinates. Most of the binary mixture simulations were initiated assuming a uniformly mixed bed. Some trial simulations, in which initial segregation was assumed, yielded identical results. The side walls were taken to be impermeable; i.e. the velocities normal to the side walls were set to zero. A constant pressure outflow condition was prescribed at the top boundary and a constant mass flow rate of the fluid was prescribed at the bottom boundary of the computational region. To obtain the solids distributions at different velocities, the superficial fluid velocity (prescribed at the bottom boundary) was varied from 2.5 to 11.5 mm/s roughly in increments of 1 mm/s. After each increase in the fluid velocity, 20 s of real time was simulated to achieve steady-state conditions; for the first step (i.e. at a fluid velocity of 2.5 mm/s), 40 s of real time was simulated.

First of all, the expansion characteristics of beds containing only glass beads and only hollow char were simulated. As the superficial fluid velocity was increased, these single component beds

Table 1. Computer simulation conditions

Particles	d_p (mm)	ρ_p (g/cm^3)
Glass beads	0.163	2.45
Hollow char	0.775	1.50
Fluid (water)	$\rho_l = 1$ g/cm^3; $\mu_l = 0.01$ g/cm s	
Bed composition		
Glass beads	100 g	
Hollow char	10, 50 or 70 g	
Superficial fluid velocities	2.5–11.5 mm/s	
Bed dimensions		
Dia	5.0 cm	
Height	30.0 cm	
Discretization parameters		
Cell sizes	Radial = 0.5 cm; axial = 1 cm	
Time step	0.01 s	

were found to expand uniformly. The computed average bulk densities of the beds ($\rho_{bk} = \rho_l \epsilon_l + \rho_k \epsilon_k$) are compared with the experimental data of Moritomi *et al.* (1982) in figure 1. The computed bulk densities of fluidized beds of glass beads agree reasonably well with experimental data at large fluid velocities. At low fluid velocities, the predicted bed expansion is greater than what is experimentally observed. The computed bulk densities of fluidized beds of hollow char agree very well with the experimental data over the full range of velocities. The simulation points, in this case, do not fall on a smooth curve because of the coarseness of the numerical grid; the same is true in the case of some of the other plots also, which will be presented later in this paper. Note that the curves in figure 1 intersect at a fluid velocity of 7.5 mm/s and, hence, we may expect granular layer inversion to occur at this velocity. At low fluid velocities, the glass beads will form the bottom layer because of their larger bulk density, whereas, at high fluid velocities, they will form the top layer.

Particle mixture simulations were carried out for three overall bed compositions given in table 1. Typical simulation results for the mixture of 100 g glass beads and 50 g hollow char are shown in figure 2. The layer of glass beads expands monotonically with increasing fluid velocity. At a fluid velocity of 10 mm/s, it can be seen to be clearly segregated at the top of the bed. The hollow char layer initially expands with increasing fluid velocity. But at a velocity slightly larger than the inversion velocity, it abruptly contracts to form a dense, segregated layer. This is typical of the inversion phenomena.

Experimental data gathered by Moritomi *et al.* (1982), are available only for the heights of the interfaces, obtained through visual observation of the fluidized bed. Figure 3 shows the comparison of experimental data with simulation results, again for the mixture of glass beads (100 g) and hollow

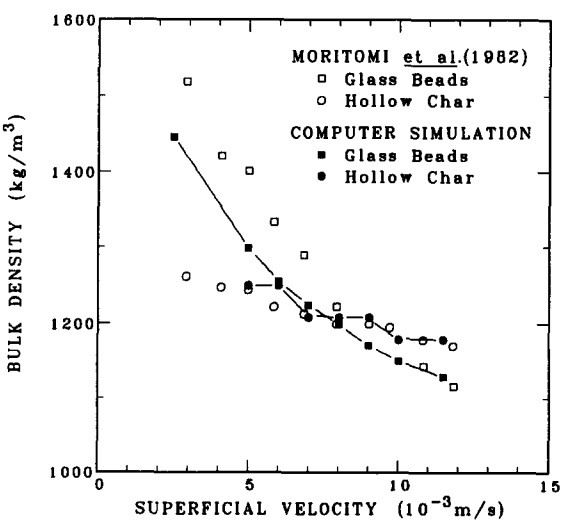

Figure 1. Bulk densities of fluidized beds of glass beads in water and hollow char in water.

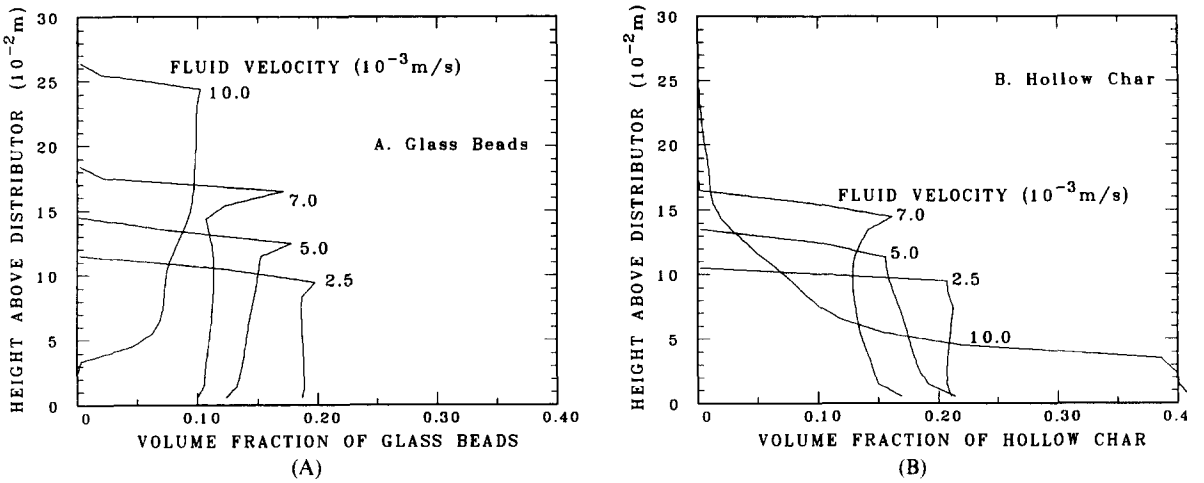

Figure 2. The volume fraction distribution of glass beads (A) and hollow char (B) close to the wall at various fluid velocities.

char (50 g). The simulated interface locations of hollow char and of glass beads were determined from plots similar to those in figure 2. The predicted expansion of the glass beads layer is greater than the experimentally observed value. Because of this over-expansion, the glass beads mix more evenly with the hollow char, and no sharp segregation pattern is observed at low fluid velocities. The expansion and the subsequent contraction of the hollow char layer, however, shows that the predicted inversion velocity is about 7 mm/s. This value is very close to the experimental data. Figure 4 shows the comparison of experimental data with simulation results for the mixture of 100 g of glass beads and 70 g of hollow char. The predicted inversion velocity is about 8 mm/s. The experimentally observed increase in the inversion velocity with the increased proportion of hollow char, appears to be discernible in the computational results. However, in view of the limited number of computations, this is not a conclusive demonstration. Simulations for the mixture of 100 g glass beads and 10 g hollow char showed that the particles remained well-mixed at all fluid velocities. Because of the very small amount of hollow char used in this case, probably the computer code was not able to resolve the hollow char layer.

So far, we have examined only the macroscopic behavior of the binary fluidized bed system. But the hydrodynamic model gives more details about the flow conditions in the bed and, as we will shortly see, the model predicts some interesting characteristics of binary fluidization such as

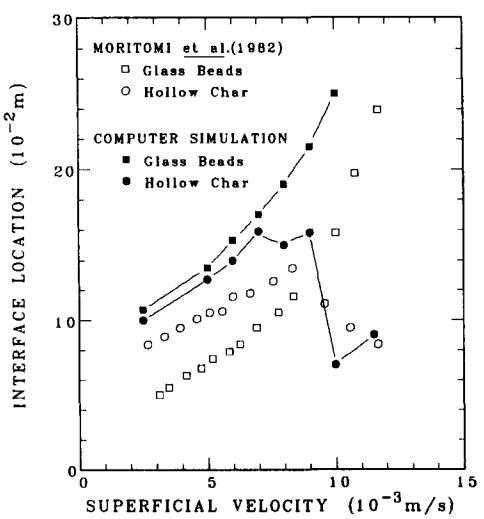

Figure 3. Expansion of a binary fluidized bed of 100 g glass beads and 50 g hollow char in water.

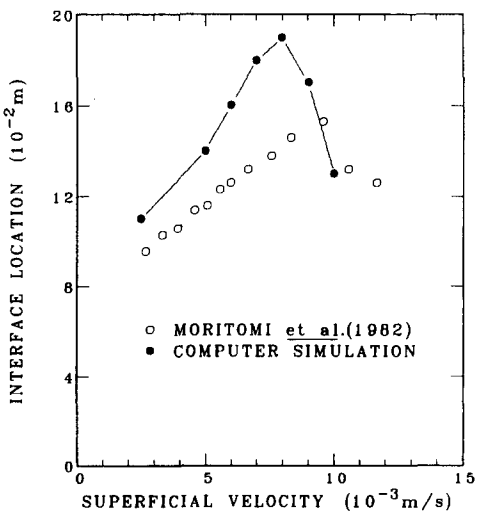

Figure 4. Expansion of the hollow char layer in a fluidized bed of 100 g glass beads and 70 g hollow char in water.

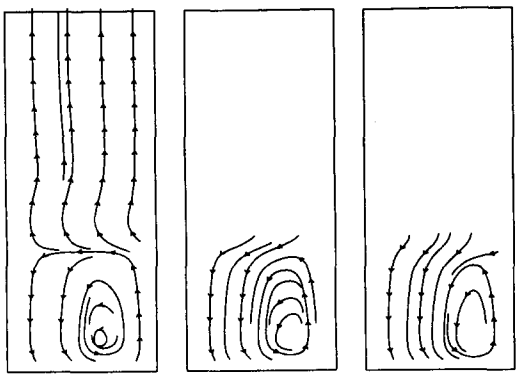

Figure 5. The streamlines at a fluid velocity of 2.5 mm/s.

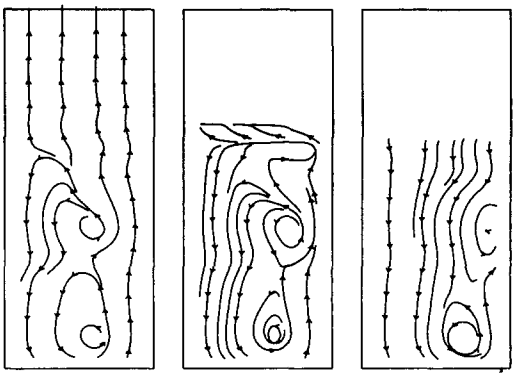

Figure 6. The streamlines at a fluid velocity of 8 mm/s.

circulation cells and radial segregation patterns. The flow patterns in the bed were studied by plotting streamlines using the NCAR Graphics Software (Henderson & Clare 1979). In the following figures the streamlines are shown on the right half of a vertical slice of the bed with an exaggerated radial dimension. Figure 5 shows the streamlines of the three phases at a fluid velocity of 2.5 mm/s for the system of 50 g hollow char and 100 g glass beads. The fluid and the particulate phases are seen to be descending at the center and ascending near the walls. Such a circulatory flow pattern was persistent over 10 s of simulation time. Surprisingly, the fluid flow direction changes very rapidly as the fluid enters or leaves the bed. The fluid flow above the bed is rectilinear and is unaffected by the circulation cell within the bed. Figure 6 shows the streamlines at a fluid velocity of 8 mm/s, which is close to the inversion velocity. The bed has expanded, but the features of the flow are similar to the previous case. Figure 7 shows the streamlines at a fluid velocity of 11.5 mm/s. The hollow char has settled to a small layer at the bottom; above that layer, however, there is a mixture layer containing a small amount of hollow char. The glass beads layer has expanded a great deal and contains two major circulation cells: one in the mixture layer and another in a layer of glass only (located above the mixture layer). The fluid has a circulation cell only in the mixture layer; in the layers containing only one component the fluid flow is rectilinear.

The simulations also show that the granular phases may segregate radially when the fluid velocity is close to the inversion velocity. Figure 8 shows the volume fraction contour plots on the right half of a vertical slice of the bed (with an exaggerated radial dimension) for glass beads and hollow char at a fluid velocity of 2.5 mm/s for the system of 50 g hollow char and 100 g glass beads. It can be seen that both the phases are nearly uniformly distributed; the hollow char, however, has a slightly larger concentration in the region close to the side wall and the bed surface. Figure 9

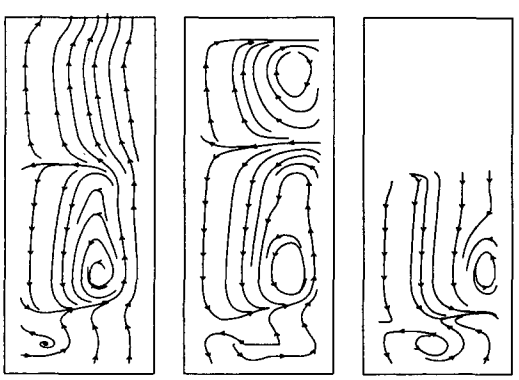

Figure 7. The streamlines at a fluid velocity of 11.5 mm/s.

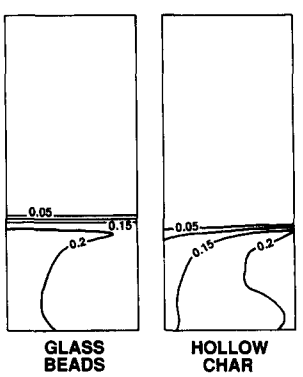

Figure 8. The solids volume fraction contour plots at a fluid velocity of 2.5 mm/s.

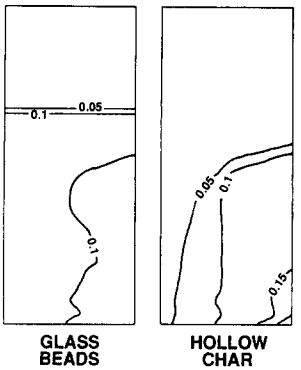

Figure 9. The solids volume fraction contour plots at a fluid velocity of 8 mm/s.

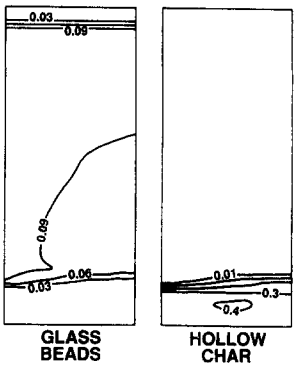

Figure 10. The solids volume fraction contour plots at a fluid velocity of 11.5 mm/s.

shows the volume fraction contour plots at a fluid velocity of 8 mm/s, which is close to the inversion velocity. In this case we can see a marked radial segregation of the solids. The hollow char particles are seen to be segregating in a region on the right-hand side of the plot, i.e. in an annular region close to the side wall. The glass beads form the central core as well as a top layer free of hollow char. In all observations through the side wall, however, this will look like a well-mixed bottom layer and a segregated top layer of glass beads. Figure 10 shows the volume fraction contour plots at a fluid velocity of 11.5 mm/s. The glass beads form a uniform top layer of the volume fraction at about 0.09 and the hollow char forms a dense bottom layer of the volume fraction at about 0.4. Moritomi *et al.* (1982), did not report any variation in the solids distribution in the radial direction. In theoretical studies, it is usually assumed that the solids are distributed uniformly in the radial direction (e.g. Gibilaro *et al.* 1986). But the simulation results show that marked radial segregation of the particulate phases is possible at a fluid velocity close to the inversion velocity. A plausible explanation for this is as follows. We saw earlier that at the point of inversion the two single-component beds have identical bulk densities. This suggests that at the point of inversion the phases may exist in any state of mixing—the radially segregated state being one of them. The steady-state solution given by the computer simulation is such a radially segregated state. At present there are no experimental data available to verify this prediction.

CONCLUSIONS

We have presented a first attempt to study segregation in a liquid fluidized bed using a multiparticle numerical model. Semiquantitative agreement with some limited experimental data has been obtained without using any adjustable parameters. The predicted inversion velocities of 7.0 and 8.0 mm/s are close to the experimental values of 7.0 and 9.7 mm/s. A small variation in the inversion velocity with respect to the overall bed composition could be discerned. However, in view of the limited number of computations, this is not a conclusive demonstration. The simulation results also give a detailed picture of the solids distribution in the bed that shows radial segregation patterns. No experimental data are available to verify these predictions.

These results increase confidence in the treatment of the gas–solid drag terms and buoyancy effects used in the model. However, further development of these constitutive laws will be required to refine the agreement with experimental data. The model should also be used to study segregation in gas fluidized beds for further verification.

REFERENCES

ARASTOOPOUR, H., LIN, D. & GIDASPOW, D. 1980 Hydrodynamic analysis of pneumatic transport of a mixture of two particle sizes. In *Multiphase Transport*, Vol. 44. Hemisphere, Washington, D.C.

DALLA VALLE, J. M. 1948 *Micromeritics*. Pitman, London.

EPSTEIN, N. & LE CLAIR, B. P. 1985 Liquid fluidization of binary particle mixtures. Part II: bed inversion. *Chem. Engng Sci.* **40,** 1517–1526.

FEDORS, R. F. & LANDEL, R. F. 1979 An empirical method of estimating the void fraction in mixtures of uniform particles of different size. *Powder Technol.* **23,** 225–231.

GARSIDE, J. & AL-DIBOUNI, M. R. 1977 Velocity–voidage relationships for fluidization and sedimentation. *Ind. Engng Chem. Process Des. Dev.* **16,** 206–214.

GIBILARO, L. G., DI FELICE, R., WALDRAM, S. P. & FOSCOLO, P. U. 1986 A predictive model for the equilibrium composition and inversion of binary-solid liquid-fluidized beds. *Chem. Engng Sci.* **41,** 379–387.

GIDASPOW, D. & ETTEHADIEH, B. 1983 Fluidization in two-dimensional beds with a jet. 2: hydrodynamic modeling. *Ind. Engng Chem. Fundam.* **22,** 193–201.

GREENSPAN, H. P. & UNGARISH, M. 1982 On hindered settling of particles of different sizes. *Int. J. Multiphase Flow* **8,** 587–604.

HARLOW, F. H. & AMSDEN, A. A. 1975 Numerical calculation of multiphase fluid flow. *J. comput. Phys.* **17,** 19–52.

HENDERSON, L. & CLARE, F. (Eds) 1979 *NCAR Graphics Software.* National Center for Atmospheric Research, Boulder, Colo.

MORITOMI, H., IWASE, T. & CHIBA, T. 1982 A comprehensive interpretation of solid layer inversion in liquid-fluidized beds. *Chem. Engng Sci.* **37,** 1751–1757.

MORITOMI, H., YAMAGISHI, T. & CHIBA, T. 1986 Prediction of complete mixing of liquid-fluidized binary solid particles. *Chem. Engng Sci.* **41,** 297–305.

NAKAMURA, K. & CAPES, C. E. 1976 Vertical pneumatic conveying of binary particle mixtures. In *Fluidization Technology* (Edited by KEAIRNS, D. L.). Hemisphere, Washington, D.C.

RIVARD, W. C. & TORREY, M. D. 1977 K-FIX: a computer program for transient, two-dimensional, two-fluid flow. Los Alamos National Lab. Report LA-NUREG-6623.

SOO, S. L. 1967 *Fluid Dynamics of Multiphase Systems.* Blaisdell, Waltham, Mass.

SYAMLAL, M. 1985 Multiphase hydrodynamics of gas–solids flow. Ph.D. Dissertation, Illinois Institute of Technology, Chicago, Ill.

SYAMLAL, M. & O'BRIEN, T. J. 1988 A generalized drag correlation for multiparticle systems. *Powder Technol.* Submitted for publication.

VAN DUIJN, G. & RIETEMA, K. 1982 Segregation of liquid-fluidized solids. *Chem. Engng Sci.* **37,** 727–733.